Available online at www.sciencedirect.com
SCIENCE DIRECT®
Journal of Solid State Chemistry 178 (2005) 3563–3570
JOURNAL OF SOLID STATE CHEMISTRY
www.elsevier.com/locate/jssc

Synthesis, crystal structure and two-dimensional infrared correlation spectroscopy of a layer-like transition metal (TM)-oxalate templated polyoxovanadium borate

Yanning Cao[a], Hanhui Zhang[a,b,*], Changcang Huang[a], Qiyu Yang[a], Yiping Chen[a], Ruiqing Sun[a], Fengli Zhang[a], Wenjun Guo[a]

[a]*Department of Chemistry, Fuzhou University, Fuzhou, Fujian 350002, PR China*
[b]*State Key Laboratory of Structural Chemistry, Fujian Institute of Research on the Structure of Matter, The Chinese Academy of Sciences, Fuzhou, Fujian 350002, PR China*

Received 12 July 2005; received in revised form 8 September 2005; accepted 11 September 2005
Available online 10 October 2005

Abstract

A novel polyoxometalate (POM) $Na_2(H_2en)_2\{(VO)_{10}[B_{14}O_{30}(OH)_2]_2\}\{Mn_4(C_2O_4)\ [B_2O_4(OH)_2]_2\}Mn(H_2O)_2\cdot(H_3O)_{12}(H_2O)_{19}$ **1** (en = ethylenediamine), which is a layer-like transition metal (TM) oxalate templated polyoxovanadium borate, has been synthesized under hydrothermal conditions and characterized by EPR, elemental analysis, thermal analysis, single crystal X-ray diffraction and 2D IR correlation spectroscopy studies, respectively. This compound crystallized in the triclinic space group $P\bar{1}$ with $a = 14.3842(4)$ Å, $b = 14.6837(3)$ Å, $c = 15.8681(4)$ Å, $\alpha = 64.48(1)^\circ$, $\beta = 64.68(1)^\circ$, $\gamma = 63.93(1)^\circ$, $V = 2596.80(11)$ Å^3 and $Z = 2$. The cluster anion with an open central cavity has a central band of ten edge-sharing VO_5 square pyramids, which is capped top and bottom by two crown-like polyborate ligands of formula $[B_{14}O_{30}(OH)_2]^{20-}$. There is a fragment of $\{Mn_4(C_2O_4)[B_2O_4(OH)_2]_2\}^{2-}$ fixed in the central cavity as a guest part. The cluster units are connected to form a two-dimensional (2D) framework by octahedral Mn(II) and Na^+ sites. In addition, we first introduce the generalized 2D correlation spectroscopy to explore the POMs and obtain the dynamic information about structural changes of POMs.
© 2005 Elsevier Inc. All rights reserved.

Keywords: Polyoxometalates; Vanadium; Borate; 2D IR correlation spectroscopy; Clusters

1. Introduction

Polyoxometalates (POMs) offer an unmatched variety of structural motifs and wide ranging applications in several areas such as catalysis, medicine, materials science, environmental decontamination, and biochemical processes [1]. Although various preparation methods have been proposed to obtain such POMs, the mechanism of formation of POMs is still not well understood and mostly described as self-assembly. Therefore, rational synthesis of novel POM architectures is a major challenge. Recently, utilizing the interaction of carboxylate-containing, organic compounds with polyoxoanions has brought a number of products [2]. On the other hand, a number of transition metal (TM)–POM hybrid compounds have already been prepared [3]. In these compounds, the TM fragments usually play two roles: (1) connect the POM cluster subunits to 1-, 2-, and even 3D extended solid frameworks, (2) occupy the lacunae on the POM cluster subunits to reproduce the mono-, di-, or tri-substituted products. Attractively, these modified products have shown great potential applications in magnetism and catalysis [4]. Therefore, finding new TM–POM hybrid compounds is one of the great challenges facing chemists.

Presently, more and more novel POMs have been synthesized, but the investigation on their capability and application have been relatively less carried on. Even though some of the POMs have been put into practice, the

*Corresponding author. Department of Chemistry, Fuzhou University, Fuzhou, Fujian 350002, PR China. Fax: 86 591 8789 3239.
E-mail address: zhanghh1840@hotmail.com (H. Zhang).

0022-4596/$ - see front matter © 2005 Elsevier Inc. All rights reserved.
doi:10.1016/j.jssc.2005.09.017

mechanism of the function of the POMs remains incompletely understood. Thus, some new technology and method are needed to resolve these problems. Generalized two-dimensional (2D) correlation spectroscopy proposed by Noda [5], which is an extension of the original 2D correlation spectroscopy, has become a very powerful and versatile tool for elucidating subtle spectral changes induced by an external perturbation such as light, heat, electricity, magnetism, chemistry, or mechanical force. It emphasizes spectral features not readily observable in conventional 1D spectra and probes the specific order of certain events taking place under the influence of a controlled physical variable. Recently, 2D-IR correlation spectroscopy has been applied extensively to protein, polymer, and medicine research [6].

We are currently interesting in combining the boron and the polyoxovanadium in the same crystalline material, which is relatively less studied [7], to generate a new class of materials with novel framework topology and properties. We have successfully synthesized and reported four polyoxovanadium borates [8]. Three of them consist of $V_{12}B_{18}O_{60}$ clusters and the other one consists of $V_{12}B_{16}O_{58}$ clusters. In this paper we present another novel polyoxovanadium borate: $Na_2(H_2en)_2\{(VO)_{10}[B_{14}O_{30}(OH)_2]_2\}\{Mn_4(C_2O_4)[B_2O_4(OH)_2]_2\}Mn(H_2O)_2\cdot(H_3O)_{12}(H_2O)_{19}$ **1** consisting of unprecedented $V_{10}B_{28}O_{74}$ clusters, which is a novel TM oxalate templated polyoxovanadium borate, and another interesting feature of **1** is that the TM moieties act as not only the linking part between the cluster units but the building part of the cluster units. Moreover, for the first time the 2D-IR correlation spectroscopy was introduced to explore the POMs and some interesting results were obtained.

2. Experimental

2.1. Materials and methods

All chemicals purchased were of reagent grades and used without further purification. Elemental analyses (C, H and N) were performed on a Perkin-Elmer 2400 CHN Elemental Analyzer. The EPR spectra were measured with a Bruker ER 420 instrument. The thermal gravimetric analyses (TGA) were performed on a Delta Series TGA7 instrument in N_2 environment with a heating rate of $10\,^{\circ}C\,min^{-1}$.

In order to obtain the 2D IR correlation spectra, a series of dynamic IR spectra were recorded in the range 4000–400 cm^{-1} on a Perkin-Elmer FT–IR spectrum 2000 spectrometers using KBr pellets. The temperature variation was controlled by a Portable programmable temperature controller (Model 50–886, Love Control Corporation) from 50 to 120 °C at intervals of 10 °C. The magnetic intensity variation was controlled by a homemade magnetic intensity controller from 2 to 20 mT at intervals of 2 mT. Before 2D calculation, each spectrum was smoothed and baseline corrected. Software used for calculation was provided by Tsinghua University.

Table 1
Crystal and structure refinement data for compound **1**

Empirical formula	$C_3H_{53}B_{16}Mn_{2.50}N_2NaO_{61.50}V_5$
Formula weight	1689.47
Space group	$P\bar{1}$ (No. 2)
a (Å)	14.3842(4)
b (Å)	14.6837(3)
c (Å)	15.8681(4)
α (deg.)	64.48(1)
β (deg.)	64.68(1)
γ (deg.)	63.93(1)
V (Å^3)	2596.80(11)
Z	2
ρ_{cal} (g cm^{-3})	2.161
μ(Mo$K\alpha$) (mm^{-1})	1.608
R_1[a] $[I>2\sigma(I)]$	0.0649
wR_2[b] $[I>2\sigma(I)]$	0.1782

[a] $R_1=\Sigma||F_o|-|F_c||/\Sigma|F_o|$.
[b] $wR_2=\{\Sigma[w(F_o^2-F_c^2)^2]/\Sigma[w(F_o^2)^2]\}^{1/2}$, $w=1/[\sigma^2(F_o^2)+(0.1224P)^2+10.7355P]$, where $P=(F_o^2+2F_c^2)/3$.

2.2. Synthesis

Compound **1** was synthesized by the hydrothermal method under autogenous pressure. In a typical synthesis, a mixture of: H_3BO_3 (1.20 g, 19.41 mmol), $VOSO_4$ (4.00 mL, 0.5 M),[1] en (0.60 mL), $H_2C_2O_4\cdot2H_2O$ (0.13 g), Mn powder (0.06 g, 1.11 mmol) and distilled H_2O (1.00 mL) was stirred to homogeneity and adjusted to pH 9.0 with NaOH. And then, the mixture was transferred into a 23 mL Parr acid digestion bomb and heated at 120 °C for 3 days. After cooling to room temperature, pure green block-like crystals are precipitated and collected by filtered (~55% yielded based on vanadium). Compound **1** is stable in air or water, but can be decomposed by H_2O_2. Anal. Found: C, 2.41; H, 2.87 N, 1.83. Calc.: C, 2.13; H, 3.14; N, 1.66%. IR (KBr pellet): $\nu=3429.63$ (s), 1648.47 (m), 1346.74 (s), 1280.71 (m), 1023.31 (s), 943.23 (s), 901.75 (m), 660.27 (m), 462.01(m) cm^{-1}.

2.3. X-ray crystallography

A green single crystal of **1** was mounted on a glass fiber. The data collection was performed on a Rigaku Weissenbery IP diffractometer with Mo$K\alpha$ radiation ($\lambda=0.71073$ Å) at 293 ± 2 K. Lp correction and a Ψ empirical absorption correction were made for the intensity data. The structure was solved by direct methods using SHELXS-97 [9(a)] and refined by full-matrix least-squares techniques using SHELXL-97 [9(b)]. All non-hydrogen atoms were treated anisotropically. Most of the water molecules are lattice

[1] The 50 mL aqueous solution of $VOSO_4$ (0.5 M) was prepared by H_2SO_4 (10 mL, 98 wt%), V_2O_5 (4.547 g, 25.0 mmol), $H_2C_2O_4\cdot2H_2O$ (4.098 g, 32.5 mmol) and distilled water in a 50 mL measuring flask.

water located between the cluster units. Hence, some of them just have partial occupation of atom sites. Therefore the total number of the water molecules is 16.5 in an asymmetry unit. Due to disorder in some water molecules and other atoms position, it was not possible to detect and refine the position of the hydrogen atoms. Some of the hydrogen atoms were generated for satisfying the charge requirements of the cluster. The hydroxyl hydrogen atoms were located by valence bond calculation [10]. The Mn(2) and Mn(3) atoms are disorder and each atom possesses two positions with occupancies given in parentheses: Mn(2A)(80%), Mn(2B)(20%); Mn(3A)(80%), Mn(3B)(20%). Further details of the X-ray structural analysis are given in Table 1. Ranges of some important bond lengths [Å] and bond angles (deg.) are listed in Tables 2 and 3, respectively.

3. Result and discussion

3.1. Crystal structure

The building block unit of **1** (Fig. 1) can be described as a cage-shaped architecture constructed by a $[\{(VO)_{10}[B_{14}O_{30}(OH)_2]_2\}]^{18-}$ cluster anion holding a fragment of $\{Mn_4(C_2O_4)[B_2O_4(OH)_2]_2\}^{2-}$. The most extraordinary feature of the building unit is the cage-shaped $[\{(VO)_{10}[B_{14}O_{30}(OH)_2]_2\}]^{18-}$ anion with an open central cavity (Fig. 2). It has a central band of ten trans edge-sharing square-pyramidal VO_5 groups ($V{=}O_t \times 1$, $V{-}O_b \times 4$), in which the V–O distances of the terminal oxygen atoms ($V{=}O_t$) range from 1.598(4) to 1.633(3) Å and those for the basal oxygen atoms ($V{-}O_b$) of the square-pyramidal VO_5 group range from 1.941(3) to 1.953(3) Å.

Table 2
Ranges of some important bond lengths [Å] for compound **1**

VO_5 pyramids[a]		BO_3 groups[b]		BO_4 groups[b]	
$V{=}O_t$	1.598(4)–1.633(3)	$B{-}O_V$	1.379(6)–1.383(6)	$B{-}O_V$	1.466(6)1.485(6)
$V{-}O_b$	1.941(3)–1.953(3)	$B{-}O_B$	1.352(6)–1.368(6)	$B{-}O_B$	1.445(6)–1.520(6)
$Mn_4O_{14}(C_2O_4)$ groups[c]		$MnO_4(H_2O)_2$ octahedra[d]		$NaO_3(H_2O)_3$ octahedra[d]	
$Mn{-}O_B$	2.073(3)–2.134(6)	$Mn{-}O_B$	2.168(3)–2.193(3)	$Na{-}O_B$	2.324(5)–2.423(5)
$Mn{-}O_{Ox}$	2.194(4)–2.305(5)	$Mn{-}O_{OW}$	2.201(5)	$Na{-}O_t$	2.275(5)
				Na–Oow	2.266(19)–2.552(15)

[a]O_t, terminal oxygen atoms of $V{=}O$; O_b, oxygen atoms in basal plan of VO_5 pyramids.
[b]O_V, oxygen atoms bridging boron and vanadium atoms in B–O–V linkages. O_B, oxygen atoms bridging boron atoms in B–O–B linkages.
[c]O_B, oxygen atoms in Mn–O–B linkages; O_{Ox}, oxygen atoms of oxalate in Mn–O–C linkages.
[d]O_B, oxygen atoms in BO_3 or BO_4 Groups; O_{OW}, oxygen atoms of water molecules; O_t oxygen atoms in $Na{-}O{=}V$ linkages. The environment of sodium ion consists in an distorted octahedron (OW(4) and OW(23) coordinated with the sodium ion are disordered).

Table 3
Ranges of some important bond angles (deg.) for compound **1**

VO_5 pyramids[a]		BO_3 groups[b]	
$O_t{=}V{-}O_b$	106.08(19)–111.39(18)	$O_v{-}B{-}O_B$	119.9(4)–122.6(4)
$O_b{-}V{-}O_b$	76.27(14)–145.98(15)	$O_B{-}B{-}O_B$	116.5(4)–119.8(4)
$Mn_4O_{14}(C_2O_4)$ groups[c]		BO_4 groups[b]	
$O_B{-}Mn{-}O_B$	80.1(3)–139.06(15)	$O_v{-}B{-}O_B$	108.3(4)–113.6(4)
$O_B{-}Mn{-}O_{o.x}$	75.56(16)–154.7(3)	$O_B{-}B{-}O_B$	103.7(3)–113.3(4)
$MnO_4(H_2O)_2$ octahedra[d]		$(C_2O_4)^{2-}$ group	
$O_B{-}Mn{-}O_B$	64.84(11)–115.16(11)	O–C–O	125.7(6)
$O_B{-}Mn{-}O_{OW}$	84.96(17)–95.04(17)	O–C–C	113.0(6)–121.3(7)
$NaO_3(H_2O)_3$ octahedra[d]		$(H_2en)^{2+}$ groups	
O–Na–O	77.9(3)–162.1(2)	N–C–C	111.6(12)–119.2(10)

[a]O_t, terminal oxygen atoms of $V{=}O$; O_b, oxygen atoms in basal plan of VO_5 pyramids.
[b]O_V, oxygen atoms bridging boron and vanadium atoms in B–O–V linkages. O_B, oxygen atoms bridging boron atoms in B–O–B linkages.
[c]O_B, oxygen atoms in Mn–O–B linkages; O_{Ox}, oxygen atoms of oxalate in Mn–O–C linkages.
[d]O_B, oxygen atoms in BO_3 or BO_4 Groups; O_{OW}, oxygen atoms of water molecules; O_t oxygen atoms in $Na{-}O{=}V$ linkages. The environment of sodium ion consists in an distorted octahedron (OW(4) and OW(23) coordinated with the sodium ion are disordered).

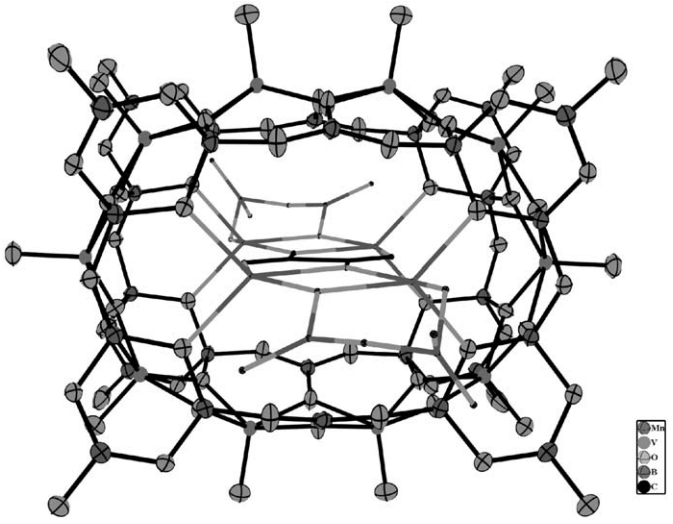

Fig. 1. A view of the $\{(VO)_{10}[B_{14}O_{30}(OH)_2]_2\}\{Mn_4(C_2O_4)[B_2O_4(OH)_2]_2\}^{20-}$ cluster unit. The $\{Mn_4(C_2O_4)[B_2O_4(OH)_2]_2\}^{2-}$ fragment is in wire representation.

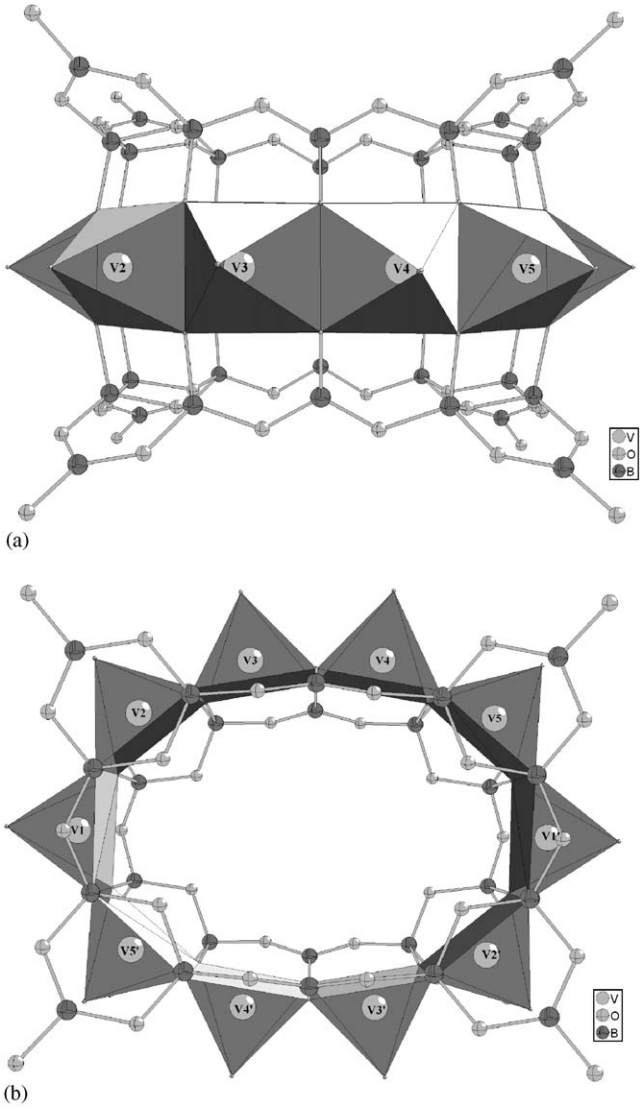

Fig. 2. (a) Side view and (b) perspective view of the $[\{(VO)_{10}[B_{14}O_{30}(OH)_2]_2\}]^{18-}$ cluster anion: the 10-membered ring of trans-edge-sharing VO_5 square pyramids is in polyhedral representation and $[B_{14}O_{30}(OH)_2]^{20-}$ ligands are in ball-and-stick representation.

The neighboring V⋯V distances range from 2.817(3) to 3.041(2) Å which imply that there may be some weak metal–metal interactions through M–O–M bridges similarly as those found in binuclear d^9 Cu(II) compounds [11]. To our knowledge, compound **1** is the first example of a POM with the planar decavanadate ring. Bond valence summations (BVSs) [10] have been applied to all the vanadium atoms and shown an average valence of about 4.24 that is close to the 4.20 expected for a V(IV) and V(V) ratio of 4:1. This also accounts for the green color of the crystals. Moreover, the EPR spectrum of **1** gives a broad signal with $g = 2.0527$, at room temperature, which also confirms the presence of V(IV) and implies the possibility of intramolecular antiferromagnetic spin coupling. Usually the reduced POMs are unstable and inclined to be oxidized in ambient atmosphere, while compound **1** can exists stably in air and in water. Following the crystal chemical classification of borates proposed by Christ, and Clark and Heller [12], the shorthand notation of the crown-like polyborate ligand is: $14{:}2[2(3{:}1\Delta + 2T) + (1{:}\Delta)]$. The $B_{14}O_{30}(OH)_2^{20-}$ ligand is formed by a ring of 8 BO_4 tetrahedra and 2 BO_3 triangles linked by corners. In the ring, a chain of 4 tetrahedra alternates with one triangle leading to a $B_{10}O_{28}$ ring. Each pair of tetrahedra within the ring shares two corners with either one BO_3 or one $BO_2(OH)$ triangle leading to the $B_{14}O_{30}(OH)_2^{20-}$ ligand. The values for B–O bonds range from 1.352(6) to 1.383(6) Å for the BO_3 triangles and from 1.445(6) to 1.520(6) Å for the BO_4 tetrahedra. Another polyborate with 14 boron atoms was recently reported in the structure of $Rb_3B_7O_{12}$ [13,14]. It is noteworthy that the polyborate results from the linkage of two B_5O_{11}, one B_3O_7 and one BO_4 groups, which are joined together by sharing corners to form sheets. The shorthand notation of the polyborate is $14{:}_\infty{}^2[2(5{:}3\Delta + 2T) + (3{:}2\Delta + T) + (1{:}T)]$. It is very interesting that the two polyborate with the same boron atoms present absolutely different structure.

It is noteworthy that the unusual $\{Mn_4(C_2O_4)[B_2O_4(OH)_2]_2\}^{2-}$ fragments are fixed in the central cavities through four pairs of Mn–(μ_3–O)–B bonds (Fig. 1). As shown in Fig. 3, the middle part of the segment is an oxalate coordinating with a pair of dimanganese (II, II) centers (the Mn(2A)–Mn(2B) distance is 3.457(2) Å) and two $[B_2O_4(OH)_2]^{4-}$ borate ligands are connected to the other side of the dimanganese centers. The similar dimanganese centers have been found in several enzymes [15], which have been motivating the synthesis and characterization of the dimanganese model compounds [16].

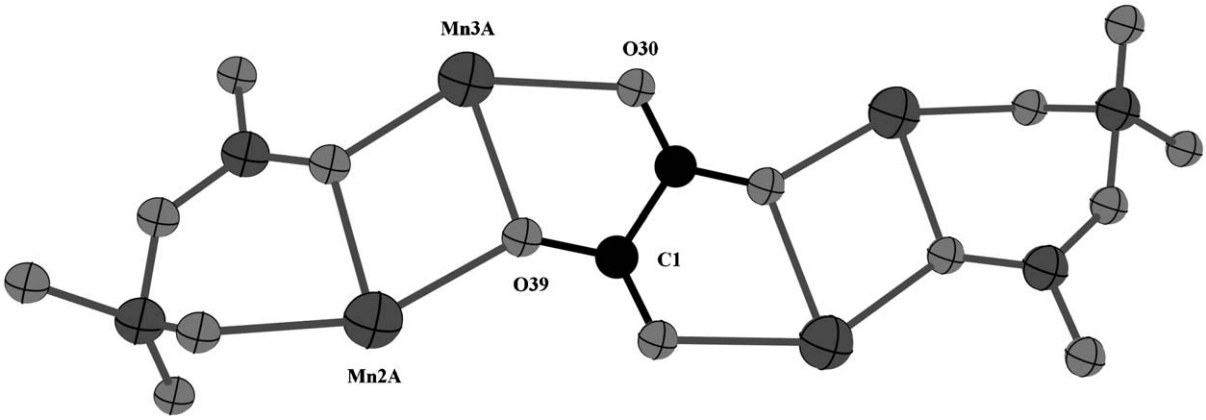

Fig. 3. A view of the fragment of $\{Mn_4(C_2O_4)[B_2O_4(OH)_2]_2\}^{2-}$.

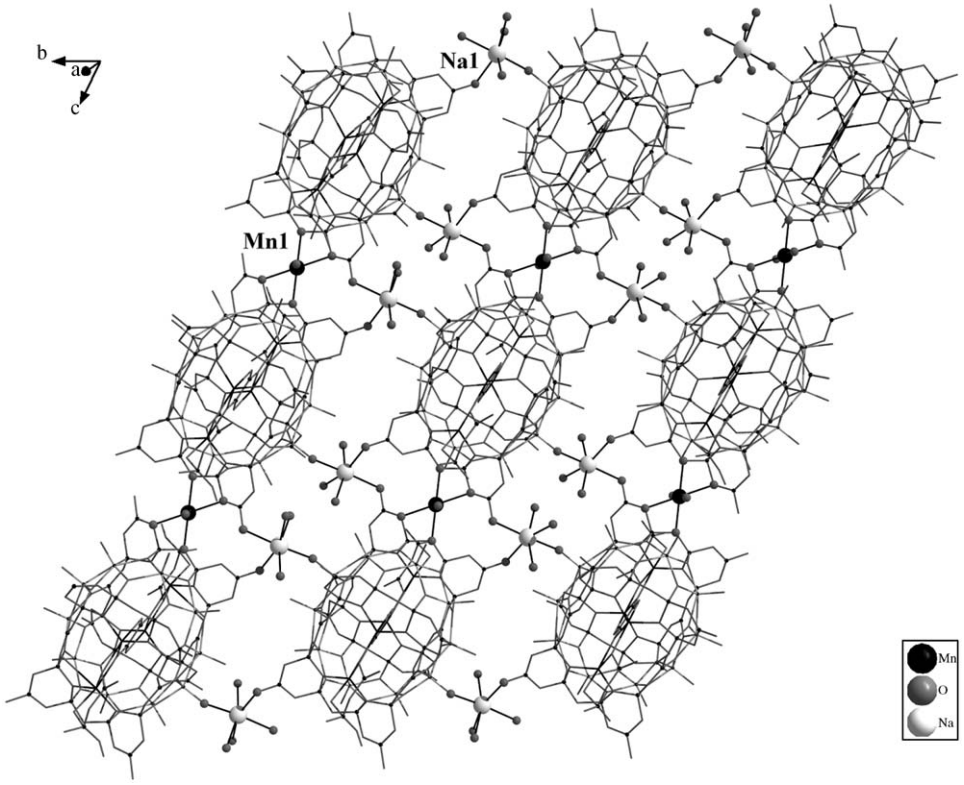

Fig. 4. Wires representation of the 2D layer structure constructed from $V_{10}B_{28}$ clusters and the octahedral Mn(II) and Na^+ sites in ball-and-stick representation. The dissociated water and en molecules between the clusters are omitted for clarity.

Another unusual feature of **1** is that two different metal sites connect the building block units to present a layer-like framework (Fig. 4). The $\{Mn(II)(H_2O)_2\}^{2+}$ sites first link the building block units into one-dimensional chains via Mn–(μ_3–O)–B bonds (Mn–O 2.168(3)–2.193(3) Å). And then, the octahedral Na^+ sites connect the chains into a layer-like framework by Na–O═V and Na–O–B (Na–O 2.275(5)–2.423(5) Å), respectively. The formation of the compound **1** is suggestive that it maybe a potential magnetic material. The ethylenediamine molecules and water molecules reside between the clusters.

3.2. IR analysis

In the IR spectrum of the compound **1**, the strong and broad band at about 3430 cm^{-1} is related to the stretch of νN–H and νO–H. The band at about 1650 cm^{-1} is ascribed to the stretch of $C=O$,δN–H and δOH. The band at 1350 cm^{-1} is due to the asymmetrical stretch of the BO_3 group. The bands at 1030 cm^{-1} are attributed to the asymmetrical stretch of the BO_4 tetrahedron. The 1000–950 cm^{-1} bands are attributed to asymmetrical stretching vibrations of the terminal V═O. The

950–880 cm^{-1} bands are assigned to the symmetrical stretching vibrations. The 600–800 cm^{-1} bands are ascribed to the stretch of symmetrical and asymmetrical V–O–V and Mn–O–B stretching. The skeletal stretching of the cluster unit presents at about 400–600 cm^{-1}.

3.3. 2D-IR correlation analysis

In order to clarify the structural changes of the cluster units in compound **1** more efficiently, 2D correlation analysis is applied in the spectral region of 400–1100 cm^{-1}. Fig. 5 shows the temperature-dependent and magnetism-dependent IR spectra of compound **1**.

Fig. 6 depicts the synchronous and asynchronous 2D correlation spectra of compound **1**. As shown in Fig. 6(a), three strong autopeaks along the diagonal line are unambiguously detected at 888, 928 and 982 cm^{-1}, which demonstrate the intensity change of V═O band is sensitive to the temperature variation. However, the positive cross-peaks at (928, 888), (982, 888) and (982, 928) cm^{-1} indicate the same direction of the intensity variations in the symmetrical and asymmetrical V═O stretching vibrations modes. The peak at 1058 cm^{-1} is ascribed to the asymmetrical stretching vibration of B–O in BO_4 tetrahedrons. So the positive sign of the cross peak at (982, 1058) cm^{-1} reveals that the direction of the V═O and B–O intensity changes are also same. In the asynchronous spectrum (Fig. 6(a)), according to the rule of Noda [5(a)], the positive sign of the cross-peak at (982, 888), (982, 928) and (982, 1058) cm^{-1} reveals that the intensity changes of V═O bands occur prior to that of the B–O bands.

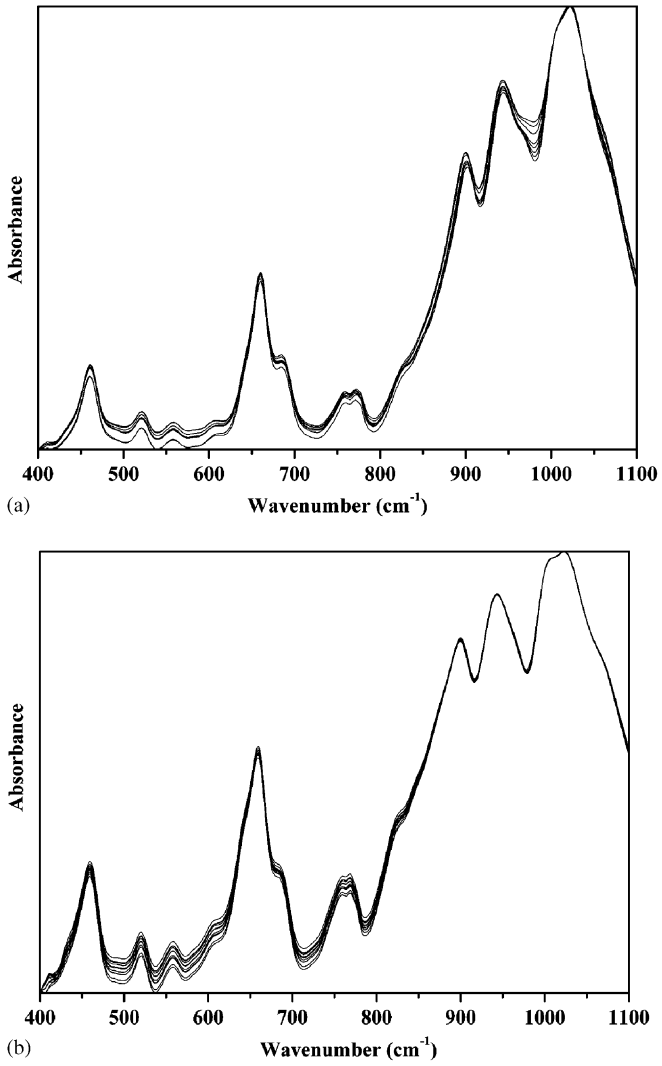

Fig. 5. (a) Temperature-dependent IR spectra of compound **1** over a temperature range from 50 to 120 °C and (b) magnetism-dependent IR spectra of compound **1** over a magnetic intensity from 2 to 20 mT.

In Fig. 6(b), there are only two main auto peak groups are observed in the band region of 460–600 and 700–850 cm^{-1} in the synchronous spectrum. In the asynchronous spectrum (Fig. 6(b)), there are only very weak cross-peaks appearing in those band regions. All these demonstrate that the intensity changes of the skeleton, V–O–V and Mn–O–B bonds are synchronized on the whole and sensitive to the magnetism variation.

From the above analyses, we can discover that in compound **1**, the intensity change of V═O band is sensitive to the temperature variation, and yet the intensity changes of skeleton, V–O–V and Mn–O–B bonds can be remarkably affected by the magnetism variation. Moreover, the intensity changes of V═O bands occur prior to that of the B–O bands in BO_4 tetrahedra during the temperature elevation. These results indicate that the subtle structural changes of POMs can be clearly probed by the generalized 2D IR correlation spectroscopy. In other words, the generalized 2D IR correlation spectroscopy can present an interesting way to check the presence or breaking of the POMs structure during the chemical reactions, which is valuable for the in-depth study of POMs, such as exploring the mechanism of POMs catalysis, researching the interaction between the building blocks of POMs.

3.4. Thermal analysis

The TG curve of compound **1** can be divided into three weight loss steps. The weight loss of 11.69% at 70–200 °C corresponds to the loss of lattice water and ligand water molecules (calc. 12.79%). The weight loss of 4.44% at 200–400 °C arises from the decomposition of en and oxalate molecules (calc. 4.44%). In the range of 400–1000 °C, the weight loss of 8.00% should correspond to the sublimation of B_2O_3 (calc. 32.97%). The lower reduction in mass loss indicates that B_2O_3 was not completely sublimated in the range of 400–1000 °C.

4. Conclusions

In conclusion, a novel polyoxovanadium borate has been synthesized by hydrothermal method. It is a TM

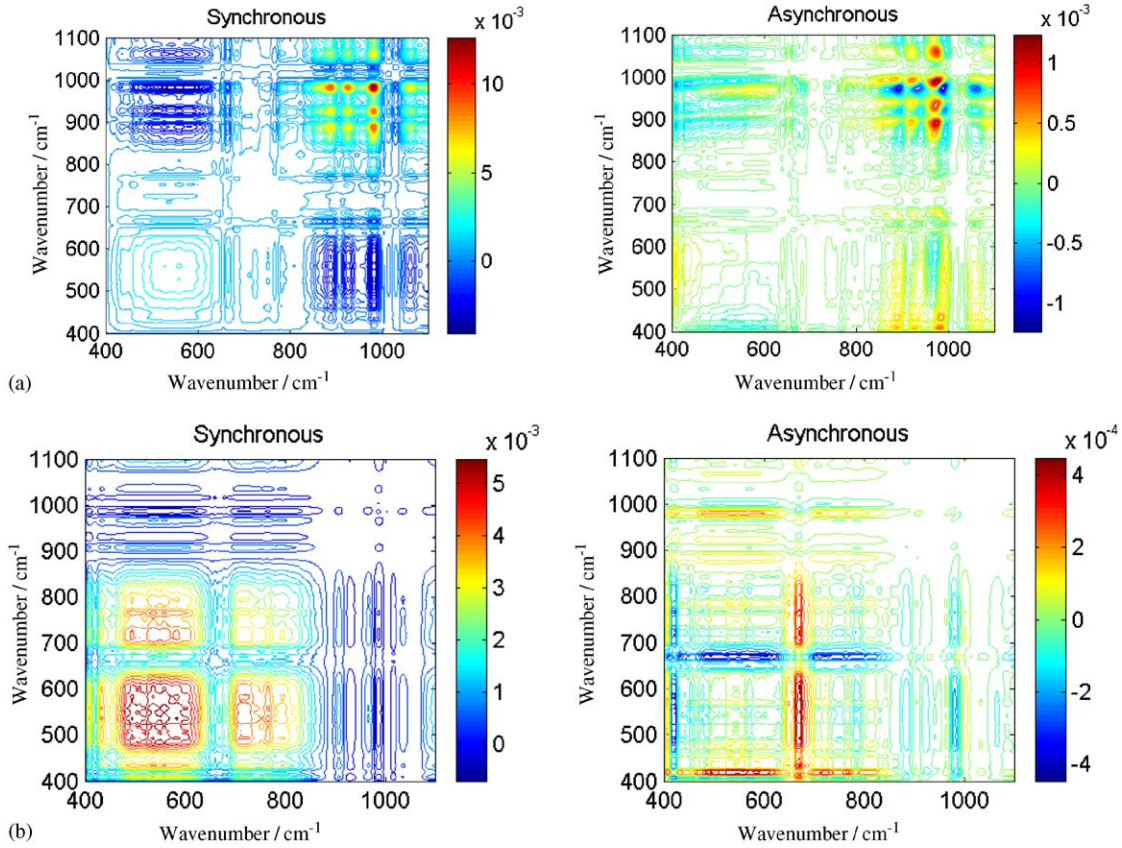

Fig. 6. Synchronous and asynchronous correlation spectra of compound **1** in the range of 400–1100 cm^{-1}: (a) over a temperature ranges from 50 to 120 °C and (b) over a magnetic intensity from 2 to 20 mT.

oxalate templated polyoxovanadium borate with a 2D layer structure constructed from unprecedented $V_{10}B_{28}O_{74}$ clusters and coordination complex fragments. The control of POMs structure by the TM oxalate reveals an interactive structural hierarchy in materials. This could open new opportunities for possible tuning of the properties and for studying structure-property relationships. Moreover, we first extend the 2D IR correlation spectroscopy to explore the POMs and it clearly probes the subtle changes of POMs induced by the temperature and magnetic intensity variations. Therefore it has the potential to become an important tool for the in-depth study of POMs.

Acknowledgments

This work was supported by the Natural Science Foundation of Fujian Province (Project no. K02028), the Foundation of Education Committee of Fujian Province (Project no. JB04049) and the State Key Laboratory of Structural Chemistry, Fujian Institute of Research on the Structure of Matter, Chinese Academy of Sciences. We thank Prof. Sun Suqin (Tsinghua University, Beijing, China) for providing the 2D IR correlation analysis software.

Reference

[1] (a) W.R. Herbert, H. Ionel, S.H. Narayan, Chem. Rev. 103 (2003) 2579;
(b) M.T. Pope, T. Yamase (Eds.), Polyoxometalate Chemistry for Nanocomposite Design, Kluwer, Dordrecht, 2002;
(c) M.T. Pope, A. Müller (Eds.), Polyoxometalates: From Topology via Self-Assembly to Applications, Kluwer, Dordrecht, 2001;
(d) E.J. Baran, J. Inorg. Biochem. 80 (2000) 1;
(e) H.T. Katherine, H.M. John, O. Chris, Chem. Rev. 99 (1999) 2561;
(f) M.T. Pope, A. Müller (Eds.), Polyoxometalates: From Platonic Solids to AntiretroViral ActiVity, Kluwer, Dordrecht, 1994;
(g) M.T. Pope, Heteropoly and Isopoly Oxometalates, Springer, Berlin, 1983.
[2] (a) S. Reinoso, P. Vitoria, L. Lezama, A. Luque, J.M. Gutiérrez-Zorrilla, Inorg. Chem. 42 (2003) 3709;
(b) B. Salifnac, S. Riedel, A. Dolbecq, F. Schéresse, E. Cadot, J. Am. Chem. Soc. 122 (2000) 10381;
(c) A. Müller, S. Sarkar, S.Q.N. Shah, H. Bögge, A.X. Trautwein, V. Schünemann, Angew. Chem. Int. Ed. 38 (1999) 3238;
(d) A. Müller, S. Polarz, S.K. Das, E. Krickemeyer, H. Bögge, M. Schmidtmann, B. Hauptfleisch, Angew. Chem. Int. Ed. 38 (1999) 3241;
(e) X. Wei, H.M. Dikman, M.T. Pope, Inorg. Chem. 36 (1997) 130.
[3] (a) M.S. Balula, J.A. Gamelas, H.M. Carapuça, A.M.V. Cavaleiro, W. Schlindwein, Eur. J. Inorg. Chem. 3 (2004) 619;
(b) X.-B. Cui, J.-Q. Xu, H. Meng, S.-T. Zheng, G.-Y. Yang, Inorg. Chem. 43 (2004) 8005;
(c) M. Yuan, Y. Li, E. Wang, C. Tian, L. Wang, C. Hu, N. Hu, H. Jia, Inorg. Chem. 42 (2003) 3670;

(d) R.S. Raring Jr., J. Zubieta, J. Solid State Chem. 167 (2002) 370;
(e) U. Kortz, S. Matta, Inorg. Chem. 40 (2001) 815.
[4] (a) V.M. Vasylyev, R. Neumann, J. Am. Chem. Soc. 126 (2004) 884;
(b) N.M. Okun, T.M. Anderson, G.L. Hill, J. Am. Chem. Soc. 125 (2003) 3194;
(c) M.A. Khenkin, R. Neumann, J. Org. Chem. 67 (2002) 7075;
(d) J.S.B. Johnson, A. Stein, Inorg. Chem. 40 (2001) 801;
(e) J.D. Aiken III, R. Finke, J. Am. Chem. Soc. 121 (1999) 8803.
[5] (a) I. Noda, Appl. Spectrosc. 47 (1993) 1329;
(b) I. Noda, Appl. Spectrosc. 54 (2000) 994;
(c) I. Noda, A.E. Dowrey, C. Marcott, G.M. Story, Y. Ozaki, Appl. Spectrosc. 54 (2000) 236.
[6] (a) S. Gnanakaran, R.M. Hochstrasser, J. Am. Chem. Soc. 123 (2001) 12886;
(b) K. Murayama, Y. Wu, B. Czarnik-Matusewicz, Y. Ozaki, J. Phys. Chem. B. 105 (2001) 4763;
(c) J. Zhang, H. Tsuji, I. Noda, Y. Ozaki, J. Phys. Chem. B 108 (2004) 11514;
(d) V.G. Gregoriou, S.E. Rodman, B.R. Nair, P.T. Hammond, J. Phys. Chem. B. 106 (2002) 11108;
(e) R. Hua, S. Sun, Q. Zhou, I. Noda, B. Wang, J. Pharm. Biol. Anal. 33 (2003) 199;
(f) Q. Zhou, S. Sun, L. Zuo, Vibrational Spectroscopy 36 (2004) 207.
[7] (a) J.T. Rijssenbeek, D.J. Rose, C. Robert, J. Zubieta, Angew. Chem. Int. Ed. 36 (1997) 1008;
(b) C.J. Warren, D.J. Rose, R.C. Haushalter, J. Zubieta, Inorg. Chem. 37 (1998) 1140;
(c) C.J. Warren, J.T. Rijssenbeek, D.J. Rose, R.C. Haushalter, J. Zubieta, Polyhedron 17 (1998) 2559;
(d) C.J. Warren, R.C. Haushalter, D.J. Rose, J. Zubieta, Inorg. Chim. Acta. 282 (1998) 123;
(e) I.D. Williams, M. Wu, H.H. Sung, X.X. Zhang, J. Yu, Chem. Commum. (1998) 2463.
[8] (a) Y. Cao, H. Zhang, C. Huang, Y. Chen, R. Sun, W. Guo, J. Mol. Struct. 733 (2005) 211;
(b) Z. Lin, H. Zhang, C. Huang, R. Sun, Y. Chen, X. Wu, Chin. J. Struct. Chem. 23 (1) (2004) 83;
(c) Z. Lin, Q. Yang, H. Zhang, C. Huang, R. Sun, Y. Chen, X. Wu, Chin. J. Struct. Chem. 23 (5) (2004) 590;
(d) Z. Lin, H. Zhang, C. Huang, R. Sun, Q. Yang, X. Wu, Acta Chim. Sin. 62 (4) (2004) 391.
[9] (a) G.M. Sheldrick, SHELXS-97, Program for X-ray Crystal Structure Solution, University of Göttimgen, Göttimgen, Germany, 1997;
(b) G.M. Sheldrick, SHELXL-97, Program for X-ray Crystal Structure Refinement, University of Göttimgen, Göttimgen, Germany, 1997.
[10] (a) I.D. Brown, K.K. Wu, Acta Cryst., Sect. B. 32 (1976) 1957;
(b) I.D. Brown, D. Altermatt, Acta Cryst., Sect. B 41 (1985) 244.
[11] (a) P.A.N. Reddy, M. Nethaji, A.R. Chakravarty, Eur. J. Inorg. Chem. 12 (2003) 2318;
(b) R.J. Doedens, Prog. Inorg. Chem. 21 (1976) 209.
[12] (a) G. Heller, Top. Curr. Chem. 131 (1986) 39;
(b) C.L. Christ, J.R. Clark, Phys. Chem. Miner. 2 (1977) 59.
[13] M. Touboul, N. Penin, G. Nowogrocki, Solid State Sci. 5 (2003) 1327.
[14] R.S. Bubnova, S.V. Krivovichev, I.P. Shakhverdova, S.K. Filatov, P.C. Burns, M.G. Krzhizhanovskaya, I.G. Polyakova, Solid State Sci. 4 (2002) 985.
[15] (a) B.S. Antharavally, R.R. Poyner, P.W. Ludden, J. Am. Chem. Soc. 120 (1998) 8897;
(b) R.S. Reczkowski, D.E. Ash, J. Am. Chem. Soc. 114 (1992) 10992;
(c) S.V. Khangulov, V.V. Barynin, N.V. Voevodskaya, A.I. Grebenko, Biochim. Biophys. Acta. 1020 (1990) 305;
(d) R. Cammack, A. Chapmann, W.-P. Lu, A.A. Karagouni, D.P. Kelly, FEBS Lett. 253 (1989) 239.
[16] (a) S. Petrie, R. Stranger, Inorg. Chem. 43 (2004) 5237;
(b) S. Mukhopadhyay, W.H. Armstrong, J. Am. Chem. Soc. 125 (2003) 13010;
(c) S. Mukhopadhyay, B.A. Gandhi, M.L. Kirk, W.H. Armstrong, Inorg. Chem. 42 (2003) 8171;
(d) T. Howard, J. Telser, V.J. DeRose, Inorg. Chem. 39 (2000) 3379.